

# The development of a vision-based system for strip position measurement during hot-strip rolling

Ben Carruthers-Watt, Cardiff University

Email: carrutherswattbn@cf.ac.uk

## 1 Introduction

### 1.1 Hot Strip Rolling

Strip steel, which is used in very wide range of applications including car body panels, white goods and cans, is manufactured in a steel rolling mill. The process involves a cast slab of steel being forced through pairs of rollers with increasingly smaller gaps until the final output thickness is achieved. There are two stages of steel rolling: hot and cold. Cold rolling is only necessary to meet certain material and thickness grades so is not performed for all strips; the material is deformed cold which reduces oxidation and resulting in an improved surface quality. Before undergoing hot rolling, the steel is pre-heated to around 1200°C in a furnace, reducing the yield strength of the material for ease of rolling. Hot rolling itself is split into two stages: roughing, where 230mm thick cast slabs are initially reduced to typically 40mm; then finishing where the final output thickness of the hot rolling mill is achieved, with typical thicknesses of between 2mm and 15mm. The work presented in this paper was performed for the finishing train of a hot strip mill, although the techniques could be relevant for other stages in the rolling process.

A finishing train consists of a series of roll stands which the strip passes through in sequence. Figure 1.1 depicts a typical layout for a 4-high rolling mill stand. The strip passes through a pair of driven work rolls to undergo deformation. The work rolls are supported by larger backup rolls to increase the stiffness and minimise unwanted work roll bending. Work rolls are often equipped with bending cylinders to further counteract bending. Atop each roll stack is a pair of actuation devices- either mechanical screws or hydraulic cylinders. These apply the necessary force to deform the strip. The roll force is then measured by a pair of load cells. The measurement system described here was developed at the Corus Port Talbot Hot Mill. The finishing train in this mill has seven four-high stands, numbered F5 to F11.

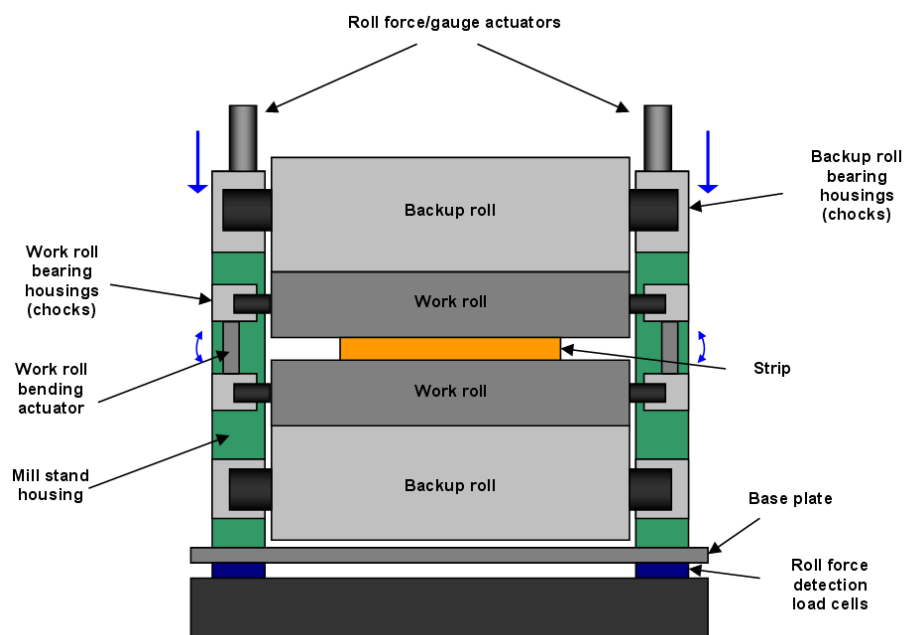


Figure 1.1: Typical layout of 4-high roll stand

## 1.2 Strip Tracking

As the steel strip passes through the finishing train, it can have a tendency towards unwanted lateral movement, known as tracking. When this tracking behaviour is particularly bad, the strip can collide with the mill and side-guides, with potentially catastrophic results. The rolls can become damaged, the edge of the strip can fold over and sometimes the strip will not enter the next roll stand, resulting in a cobble, where the strip bunches up in the inter-stand space. All of these eventualities result in maintenance and downtime, and a reduction in the quality and productivity of the mill. To prevent the collisions, the strip can be steered back to the centre line by adjusting the roll gap on one side (the “mill tilt”). The effect of this is differential deformation across the strip width, with the thinner side having additional elongation. With one edge longer than the other, a curvature is induced in the strip, steering it towards the desired path.

Strip steering is traditionally performed by the operators who manually adjust the tilts when they observe the strip deviating from the centreline. The operators are located in a pulpit viewing the mill from the side so sometimes they cannot see or act fast enough to correct the deviation. This process can be automated within the control system but first a method to measure strip position is required. Automatic control of strip steering is often achieved using differential force measurements in the roll-stand. A number of papers exist describing various control strategies based on differential force measurements [1]-[3]. However, force measurements from the load cells are not always reliable and the relationship between strip position and differential force is highly non-linear, so complex system models are required [3]. To avoid the complexities of a force-based measurement system, a direct measurement, such as a vision system, is preferred [4]. Using a camera-based system within the aggressive environment present in a steelworks can be a challenge to equipment longevity and measurement accuracy. However, by using robust image analysis processes and with adequate protection of hardware, vision systems have previously been successful in a variety of tasks in hot rolling mills [5],[6].

This paper presents a camera-based measurement system and image analysis software, suitable for overcoming the challenges of operating in the noisy and dirty environment of a steelworks.

## 2 Measurement System Design

### 2.1 Overall Design

The strip tracking measurement system is based around a vision system. It uses cameras to view the strip from the gantry above to capture images as the strip exits the roll bite. Data from the cameras is transmitted to an industrial computer via Gigabit Ethernet (GigE). The industrial computer runs bespoke image analysis software, specifically designed for this application by the author. The strip position measurements can then be output in the form of analogue voltages to a separate data logger or control system as required. The configuration of the system is essentially as a stand-alone sensor. An overview of the design is shown in Figure 2.1. The items marked with dotted lines (external system and control) do not fall under the specifications of this measurement system, but this system was designed with the capability to expand into a final control system as shown.

The design depicted here describes a 2-camera system with control on the first two stands of the finishing train, although the system has the capability to expand to the full 7 stands in the Port Talbot mill. The effectiveness of a full control system is dependant on the number of stands that are equipped for measurement.

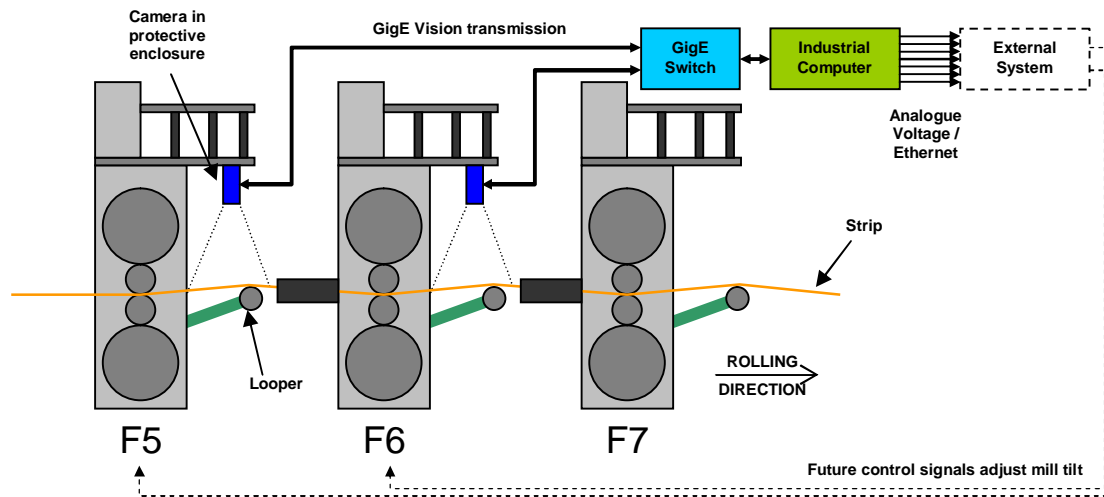


Figure 2.1: Layout of measurement system design

## 2.2 Hardware

### 2.2.1 Cameras

The cameras specified for this system design are from the Basler Scout GigE Vision series, although any GigE compatible camera can be used. GigE was used as the transmission medium because it offers 100 metres transmission at high speeds in noisy environments, exceeding the transmission capabilities of the alternatives [7] and allowing the use of standard network components and CAT 6 network cabling. The choice of camera is a trade-off between image acquisition speed and resolution; a higher resolution camera could not acquire an image as fast as a lower resolution one but measurement accuracy suffers with higher speed. Each camera was fitted with an infrared (IR) filter to minimise pixel bleeding and to protect the internal electronic components.

### 2.2.2 Computing System

The core computing system handles the measurement of strip position by performing the image processing task and output the strip position and other information as analogue voltages. The system is based around a National Instruments (NI) PXI system [8] running bespoke software created specifically for this task and the challenges involved. The core system is a Real-Time (RT) controller with a quad-core 2.2GHz processor. The RT platform was chosen to allow all processor resources to be allocated to the image analysis task and to eliminate unwanted interruptions from other sources, as would be the case with a user-interface oriented operating system such as Microsoft Windows. The high-speed multi-core processor allows parallel data processing operations to be undertaken simultaneously, resulting in a robust, high-speed measurement system. Two signal acquisition cards were selected on top of the core processing unit, mounted into a 4-slot chassis, leaving one space free for further expansion if required.

A single port GigE card was chosen for the camera interface, which links the PXI to the cameras via an 8-port GigE switch, facilitating a total of 8 cameras to be interfaced with this system.

A 32-channel analogue output board was selected for data output and integration into the mill. Multiple channels allow a large range of measured data and condition signals to be relayed to the control and data logging systems, and leaves room for future expansion. This module is equipped with standard BNC connectors for ease and security of external connections.

### 2.2.3 Location and Mounting

The cameras are positioned below the gantry above the roll-stand exit on stands F5 and F6 (the first two finishing stands) in the Port Talbot hot strip mill, as shown in Figure 2.1. Each camera is enclosed within a cooled enclosure to protect the camera electrical equipment from the heat in the mill. The enclosures specified are VideoTec NXW stainless steel water-cooled enclosures [9] with Vicor glass, specially designed for high-temperature environments. This enclosure has an air barrier, preventing dust and other deposits accumulating on the glass front, maintaining a clear view

## 2.3 Software

### 2.3.1 Overview

Previously, a piece of software was created by the author in order to analyse the location of a strip, given images recorded in the Corus Llanwern Hot Strip Mill [10]. This piece of software used simple edge detection techniques to find a straight edge in a small section of an image and output the location of this edge. The software was built using standard image analysis tools available in the National Instruments LabVIEW (a graphical programming tool) image processing toolkit and proved to be very effective for the purpose. The idea behind developing this piece of software was to prove the concept of using image analysis for strip position measurement.

The images used in the development of the original software were from the exit end of the mill, where there is not a lot of cooling water and hence not a great deal to obscure the vision of the camera. Since that software was developed, it was found that the ideal location of the cameras was towards the beginning of the mill, not at the exit [11]. A further camera was installed, this time in the Port Talbot Hot Strip Mill on the first stand, where there is considerably more cooling water, as shown in Figure 2.2.

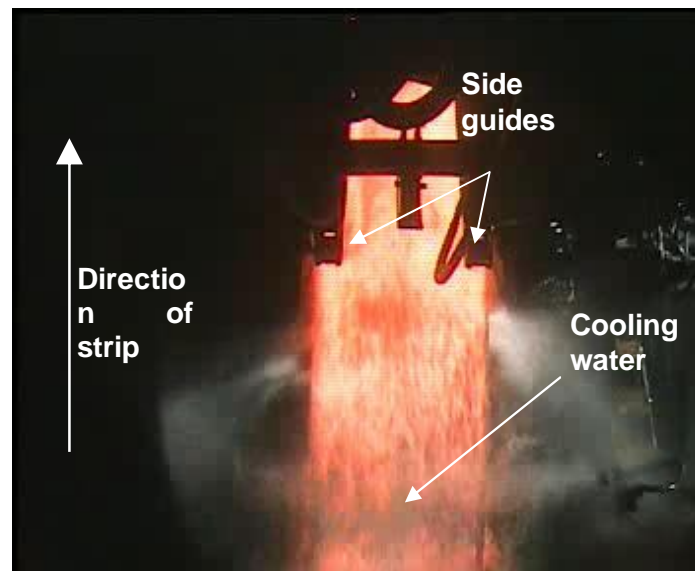


**Figure 2.2: Image from Port Talbot Hot Strip Mill, 1<sup>st</sup> stand**

When these images were run through the original software it became evident that it was not suitable for the task when there was a considerable amount of water. There became a need to develop the software in order to improve the capability and be able to process the images despite the water.

The aim of the measurement software was to determine the location of the strip centreline as close to the rolls as possible. In the image shown in Figure 2.2 the rolls are towards the bottom edge of the image. The problem with measurement occurred because the concentration of water is highest at the point where measurement is desirable due to the cooling header spraying at the exit of the roll stand. It

was thought that by fitting a line to the entire visible section of the strip, the position at the required point could be derived despite the cooling water.

The looper roller, which rises and falls to maintain strip tension, causes an apparent curvature in the strip images due to perspective effects. This apparent curve means a straight line cannot be used to fit the strip edge, instead a curve is required. The perspective effect causes a simple curve, generally with a single apex such as a quadratic. To improve the quality of fit, a cubic function was chosen which could better follow the edge of the strip if it did not fit a perfect quadratic. The curve chosen for the job was a cubic Bezier curve. Following work by O’Leary [5], a method using Bezier curve fitting to the strip edges was developed and described throughout section 2.3.

### 2.3.2 Methodology

#### Basic Edge Detection

An edge is defined as a part of an image where pixel brightness changes significantly. In mathematical terms, for a greyscale U8 (unsigned 8-bit) image, each pixel is represented as a single byte; a number from 0 to 255 where 0 is black and 255 is white. Therefore, an edge can be defined as the maximum change in value between adjacent pixels, or the maximum gradient. The task for the edge detection component of the software is to identify significant edges along the search line. For example, consider the section of a strip image shown in Figure 2.4(A). The search line is the thick green line in the centre of the rectangular search area.

To find the gradient of the pixel values, the data must be differentiated. In an image that has a tendency to be noisy such as this, then taking the gradient value across a range of pixels helps to filter out the noise. A kernel is used to apply the calculation across a number of pixels. The pixel values of the example search line are shown in Table 2.1 and an example kernel in Table 2.2.

**Table 2.1: Pixel values along search line**

Pixel Values																																					
27	30	31	31	34	37	40	40	41	49	51	51	61	58	69	59	85	140	144	159	162	171	191	193	200	200	206	202	199	204	201	196	201	200	200	199	198	197

**Table 2.2: Example gradient kernel**

Kernel								
1	1	2	2	0	-2	-2	-1	-1

The kernel is centred on the target pixel and the values are cross-multiplied with corresponding pixel values, the result is summed to find a gradient indicator at that point. It should be noted that the kernel method does not find the true gradient at that point, but a scaled indication of the gradient. The values in the kernel apply different weightings to cells dependent on their proximity to the target pixel. The kernel can be fine-tuned to suit the need of the situation and the size expanded to offer a greater amount of filtering to the pixel values. The application of the kernel is demonstrated in Table 2.3.

**Table 2.3: Application of kernel to calculate pixel gradient**

<b>Pixel Values</b>	41	49	51	51	61	58	69	59	85	
<b>Kernel</b>	1	1	2	2	0	-2	-2	-1	-1	<b>Sum (Gradient)</b>
<b>Multiple</b>	41	49	102	102	0	-116	-138	-59	-85	<b>-104</b>

This can be applied to the entire section of pixel values and is shown in Table 2.4.

**Table 2.4: Pixel Gradient Indicators**

Pixel Gradients																																					
0	0	0	0	-54	-59	-58	-63	-81	-84	-91	-85	-104	-157	-232	-387	-514	-524	-426	-338	-286	-242	-223	-163	-112	-71	-23	2	9	13	20	10	0	6	0	0	0	0

When viewed graphically, the pixel gradient indicators show the position of the edge as the turning point on the graph shown in Figure 2.3.

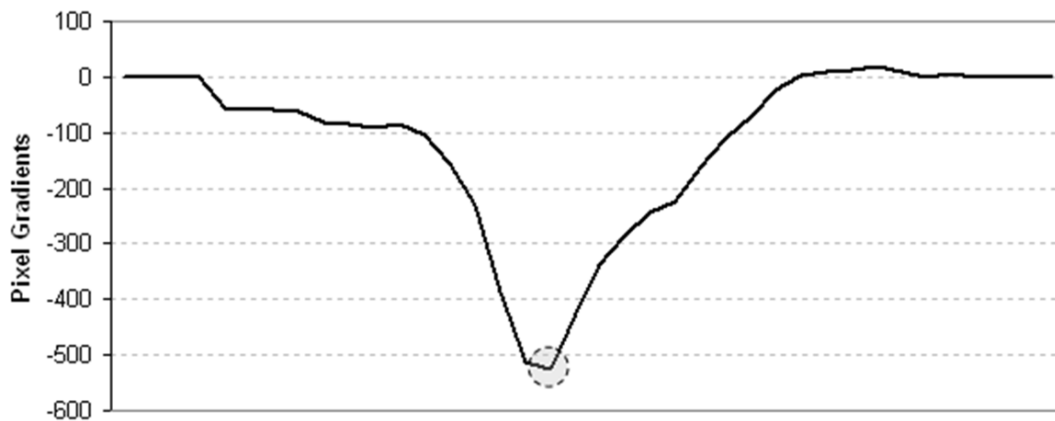


**Figure 2.3: Pixel intensity gradients along search line**

This turning point is identified where the graph in Figure 2.3 has a differential of zero. This can be found by performing a discrete differentiation on the gradient data and the result shown in Table 2.5.

**Table 2.5: Differential of pixel gradients**

Gradient of "Pixel Value Gradients" Graph																																					
0	0	0	0	-54	-5	1	-5	-18	-3	-7	6	-19	-53	-75	-155	-127	-10	98	88	52	44	19	60	51	41	48	25	7	4	7	-10	-10	6	-6	0	0	0

Note that as this is using discrete values, the zero point does not necessarily occur at a pixel site. To determine edge location, the points where the data crosses between negative and positive are deemed to contain the zero value then linear interpolation performed to find the zero-crossing point. By following this process, the cells marked in grey in Table 2.5 have been identified as "edges". Working up to this point in reference to the example image, edges are shown as red dots in Figure 2.4(B).

The process so far has identified a large number of edges, including the main strip edge. This is due to small variations in pixel values along the search line. To isolate the noisy edges from the true strip edge (highlighted darker grey in Table 2.5) a simple threshold can be applied to the pixel gradients, rejecting any edge whose pixel gradient does not have an absolute magnitude greater than, for example, 150. After applying the threshold, the true edge is identified and the result shown in Figure 2.4(C).

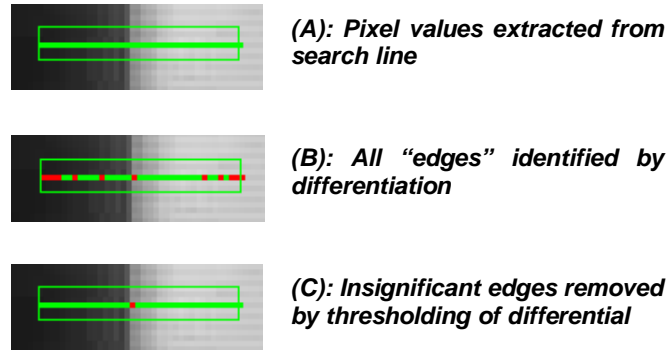


Figure 2.4: Complete basic edge detection process

### Strip Edge Identification

The example shown in Basic Edge Detection is a very "clean" section of image. The nature of this application means there are very noisy images and many false edges are identified. The thresholding process described above can only account for the worst of the false edges and other noise must be additionally removed. Figure 2.5(A) shows an example image that has undergone the aforementioned edge detection, with a threshold value of 150. Search lines have been omitted for clarity in this example image. Whilst a significant proportion of "edges" have been filtered out, there are still groups of edges seen from steam and spray in the image.

These unwanted edges are ignored by using past information about the strip edge location. Using the fitted curve from the previously analysed image, the expected edge position can be calculated for each search line. A threshold of, for example, 3 pixels can be applied to the data and any points outside that range rejected. In some cases, multiple edges may be identified with the tolerances on one search line. In these cases the average pixel position for the group is taken. By allowing two sets of acceptable regions, representing both edges of the strip, two distinct groups of pixels can be identified to which curves can be fitted. The result of this process can be seen in Figure 2.5(B). In this example, the group of pixels on the left edge are marked in yellow and the group on the right marked in blue. The red pixels show the rejected edges.

With the image processed now to a point where the edges are grouped into sets representing the two edges of the strip, a curve can be fitted to the data to find the location of the complete edge.

A Bezier curve [12] of degree  $n$  can be defined by equation (1). A cubic Bezier curve (order  $n = 3$ ) is therefore defined by equation (2)

$$B(t) = \sum_{i=0}^n \frac{n!}{i!(n-i)!} (1-t)^{n-i} t^i \mathbf{P}_i, \quad t \in [0,1] \quad (1)$$

$$B(t) = (1-t)^3 \mathbf{P}_0 + 3(1-t)^2 t \mathbf{P}_1 + 3(1-t) t^2 \mathbf{P}_2 + t^3 \mathbf{P}_3 \quad (2)$$

$\mathbf{P}_0$  to  $\mathbf{P}_3$  are points, or “knots”, defining the curve and can be of any dimension, as long as they are all the same order of dimension. In this case the requirement is to fit a curve to known points in 2-dimensional space, therefore knots  $\mathbf{P}_i = \mathbf{P}_i[x, y]$ .

The images were scanned in series of even steps down the y-axis, a total of  $m$  steps, i.e.  $m$  data points of  $y_j = y_0, y_1, \dots, y_m$ . Therefore, all the values of  $\mathbf{P}_i[y]$  are defined by a uniform spread shown in (3)

$$\mathbf{P}_i[y] = y_0 + i \frac{y_m - y_0}{n}, \quad i = 0, 1, \dots, n \quad (3)$$

The task here is to find values for  $\mathbf{P}_i[x]$ , using the least squares method.

The points along the curve are valid for  $0 \leq t \leq 1$ , however the data points from the image analysis process are defined by the y-values of the search line. Equation (4) defines how each point is mapped to a corresponding value of  $t_j$ .

$$t_j = \frac{y_j - y_0}{y_m - y_0} \quad (4)$$

The least squares method [13] minimises an error function defined as the square of the error between the curve and the true edge point,  $x_j$ . For this application the error function  $R^2$  is defined as

$$R^2 = \sum_{j=0}^m [x_j - B(t_j)]^2 \quad (5)$$

$$R^2 = \sum_{j=0}^m [x_j - ((1-t_j)^3 \mathbf{P}_0[x] + 3(1-t_j)^2 t_j \mathbf{P}_1[x] + 3(1-t_j) t_j^2 \mathbf{P}_2[x] + t_j^3 \mathbf{P}_3[x])]^2 \quad (6)$$

The method is looking for the minimum change in error for a change in  $\mathbf{P}_i[x]$ , therefore a point where the partial derivatives of  $R^2$  with respect to  $\mathbf{P}_i$  are zero,

$$\frac{\partial(R^2)}{\partial \mathbf{P}_i[x]} = 0 \quad (7)$$

$$\frac{\partial(R^2)}{\partial \mathbf{P}_0[x]} = -2 \sum_{j=0}^m [(x_j - ((1-t_j)^3 \mathbf{P}_0[x] + 3(1-t_j)^2 t_j \mathbf{P}_1[x] + 3(1-t_j) t_j^2 \mathbf{P}_2[x] + t_j^3 \mathbf{P}_3[x])) (1-t_j)^3] = 0 \quad (8)$$

$$\frac{\partial(R^2)}{\partial \mathbf{P}_1[x]} = -2 \sum_{j=0}^m [(x_j - ((1-t_j)^3 \mathbf{P}_0[x] + 3(1-t_j)^2 t_j \mathbf{P}_1[x] + 3(1-t_j) t_j^2 \mathbf{P}_2[x] + t_j^3 \mathbf{P}_3[x])) 3(1-t_j)^2 t_j] = 0 \quad (9)$$

$$\frac{\partial(R^2)}{\partial \mathbf{P}_2[x]} = -2 \sum_{j=0}^m [(x_j - ((1-t_j)^3 \mathbf{P}_0[x] + 3(1-t_j)^2 t_j \mathbf{P}_1[x] + 3(1-t_j) t_j^2 \mathbf{P}_2[x] + t_j^3 \mathbf{P}_3[x])) 3(1-t_j) t_j^2] = 0 \quad (10)$$

$$\frac{\partial(R^2)}{\partial \mathbf{P}_3[x]} = -2 \sum_{j=0}^m [(x_j - ((1-t_j)^3 \mathbf{P}_0[x] + 3(1-t_j)^2 t_j \mathbf{P}_1[x] + 3(1-t_j) t_j^2 \mathbf{P}_2[x] + t_j^3 \mathbf{P}_3[x])) t_j^3] = 0 \quad (11)$$

Equations (7) to (11) can be rearranged into matrix form and the result shown in (12)

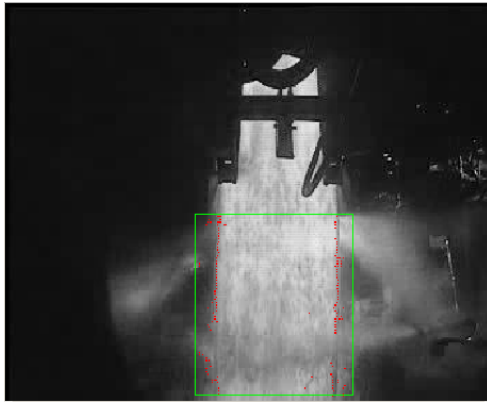
$$\begin{bmatrix} \sum_{j=0}^m (1-t_j)^6 & \sum_{j=0}^m 3(1-t_j)^5 t_j & \sum_{j=0}^m 3(1-t_j)^4 t_j^2 & \sum_{j=0}^m (1-t_j)^3 t_j^3 \\ \sum_{j=0}^m 3(1-t_j)^5 t_j & \sum_{j=0}^m 9(1-t_j)^4 t_j^2 & \sum_{j=0}^m 9(1-t_j)^3 t_j^3 & \sum_{j=0}^m 3(1-t_j)^2 t_j^4 \\ \sum_{j=0}^m 3(1-t_j)^4 t_j^2 & \sum_{j=0}^m 9(1-t_j)^3 t_j^3 & \sum_{j=0}^m 9(1-t_j)^2 t_j^4 & \sum_{j=0}^m 3(1-t_j) t_j^5 \\ \sum_{j=0}^m (1-t_j)^3 t_j^3 & \sum_{j=0}^m 3(1-t_j)^2 t_j^4 & \sum_{j=0}^m 3(1-t_j) t_j^5 & \sum_{j=0}^m t_j^6 \end{bmatrix} \times \begin{bmatrix} \mathbf{P}_0[x] \\ \mathbf{P}_1[x] \\ \mathbf{P}_2[x] \\ \mathbf{P}_3[x] \end{bmatrix} = \begin{bmatrix} \sum_{j=0}^m (1-t_j)^3 x_j \\ \sum_{j=0}^m 3(1-t_j)^2 t_j x_j \\ \sum_{j=0}^m 3(1-t_j) t_j^2 x_j \\ \sum_{j=0}^m t_j^3 x_j \end{bmatrix} \quad (12)$$

$$\equiv \begin{bmatrix} \mathbf{T} \end{bmatrix} \times \begin{bmatrix} \mathbf{P} \end{bmatrix} = \begin{bmatrix} \mathbf{X} \end{bmatrix} \quad (13)$$

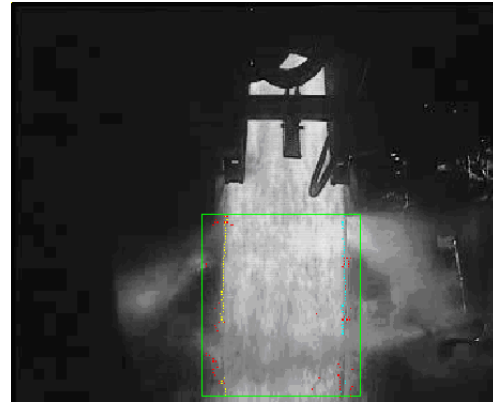
By representing (12) as (13), the values of  $\mathbf{P}_i[x]$  can then be found by evaluating (14)

$$\mathbf{P} = \mathbf{T}^{-1} \times \mathbf{X} \quad (14)$$

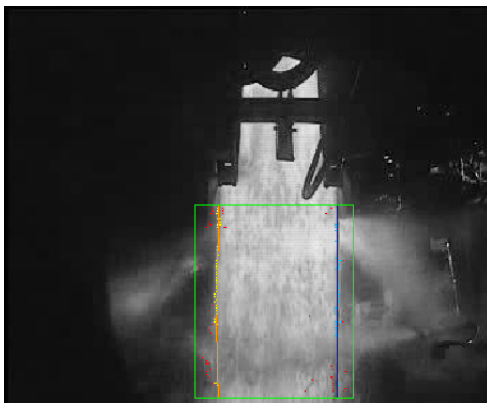
Applying this method to the point sets shown in Figure 2.5(B), the edge of the strip could be clearly identified, as shown in Figure 2.5(C). The knots can then be averaged to find a Bezier curve defining the centre-line of the strip, show in Figure 2.5(D).



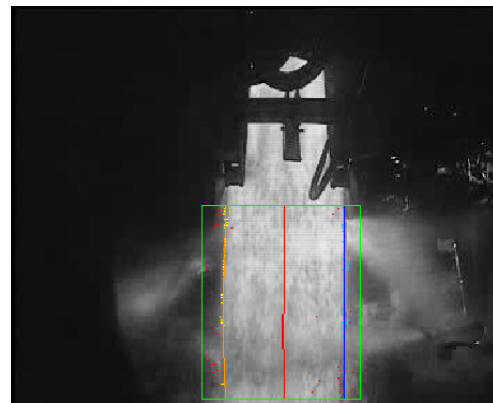
**A: All significant edges (red dots) within search window (green rectangle) identified.**



**B: Two groups of acceptable edges extracted using past edge location (yellow and blue dots)**



**C: Bezier curves fitted to acceptable edge groups using least-squares method to identify strip edges (yellow and blue lines)**



**D: Strip centreline identified as average of left and right edges (red line)**

**Figure 2.5: Complete strip edge identification process**

### **Tolerances for improving line fit**

The processed images presented in the above were subjected to a degree of limitation on the placing of points and curves. The “Acceptable Point” tolerance of a few pixels has already been discussed in the section Basic Edge Detection but further limitation is applied to the curve location to enhance the correct edge identification.

The first condition is a boundary condition, limiting the overall placement of the curve. The strip runs between guides and the camera is in a fixed location, therefore the edge will always lie within a given section of the image. The expected location of the edge is set in software and a wide boundary given, in this case 10 pixels each side, limiting the position of the curve. This boundary condition prevents the curve “running away” if there are consistently bad edges detected.

The second condition imposed on the curve effectively limits the “straightness” of the curve. This limits the location of the knots depending on the average of all calculated knot positions. The limit is applied separately for endpoint knots and mid-section knots. The endpoint knots are limited to a given number of pixels each side of the average, the mid-section knots are limited to double this value each side. The difference is applied because the mid-section knots lie further out than the curve itself. In this example the limit was set to 2 (4 for mid-section) pixels either side. This limit is applied to

prevent anomalous edges pulling a section of curve outwards away from the strip edge, and then further affecting the acceptable region for subsequent images.

The application of these limits dramatically improves the reliability and robustness of the analysis.

### **2.3.3 Evaluation of Strip Edge Detection Image Analysis Method**

The methods used to measure the strip edge position all contribute to the success of the software and work together for optimal results.

By measuring the position down the entire length of the strip, as much data as possible can be found about the shape and position of the strip in the mill. Utilising existing knowledge on the position of the strip as an edge-rejection method allows filtering of the data points which can then be used to fit a cubic Bezier curve, interpolating the missing positions. The least-squares method used to fit the curve is a straightforward matrix multiplication, requiring no iterative process, optimising processing time.

The use of tolerances and limits is the key to the successful operation of this software and hence there is a requirement to set these to reasonable values for the application.

The first tolerance that is used is the “Acceptable Point Tolerance”, defining how far an edge on a given search line may be from that in the previous image. This limit is designed to filter the random edge noise from small amounts of spray that appear in the measurement area. If this value is set too low then any strip movement will not be detected, however too high and steam around the strip will be considered to be the edge. A value of 2-3 pixels has shown to work effectively for the given data.

The curve bound tolerance limits the space in which the curve can be determined to be. This allows a reasonable working space but prevents the edge to be determined to be too far from the expected position. This bounding proves to be very effective in the case of total loss of strip image, such as in between strips passing through the mill. This limitation allows the system to recover rapidly from these situations and resume measurement very quickly. The bounding size does not have a big impact on the general operation of the software, but if it is set too low then the strip may move out of the working area of the curve. Likewise, the expected position must be a reasonable average strip position to ensure even bounding on both edges of the strip. If this value is set too high then it does allow the curve to wander too far from the expected position and the software cannot recover after losing strip images.

The straightness tolerance has proven to be the most effective method in maintaining good measurements and ignoring steam and spray. This applies a limitation on how far the curve can deviate from a straight line, preventing patches of steam and spray pulling sections too far from the correct line. A value of 2-3 pixels has proven to be effective for this example. Too low and the curve is limited to a straight line, too high and steam and spray begin to be interpreted as strip edge.

Note that all of these settings are dependent on camera resolution. During the development of the software techniques a relatively low-resolution camera of 352x288pixels (px) was used. For the full installation of an on-plant measurement system, the camera would be a higher resolution of around 700x500px. Additionally, the area of view is likely to be closer on the strip. These factors mean that each pixel will represent less physical space so the tolerance values would likely be higher.

To evaluate the effectiveness of the software, a set of images were analysed by the software to determine the centreline point at the bottom of the region of interest. These were compared to centreline positions determined by a human observer. The absolute errors between observer measurements and software measurements were calculated and the distribution plot shown in Figure 2.6. The accuracy of human observer measurements is estimated to be 0.5-1px.

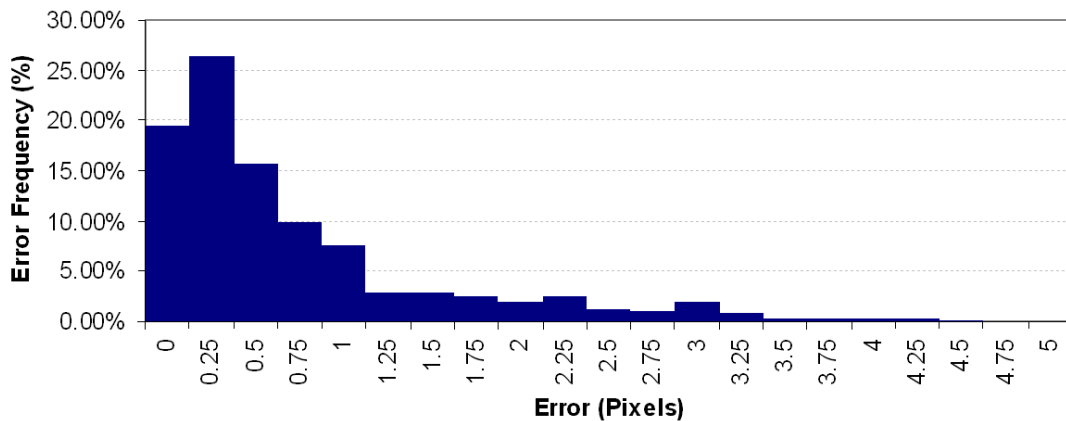


**Figure 2.6: Distribution of errors between observer and software**

The pixel resolution for the images used in this study is estimated at 13mm/px, and in a full install a resolution of around 3mm/px would be expected for a 640px camera viewing a 2m width.

The results from this study have shown that 90% of the time, measurements were determined to be within 2px accurate, relating to about 26mm in this study, or 6mm in a full installation. It is worth noting that the width of a strip is likely to vary by 6mm along the length at the exit of the mill. 80% of the results were better than 1px and 60% better than 0.5px or 1.5mm.

In the worst-case situations, errors of 3-4px were seen. These occurred in extremely obscured images and in very few cases with only 5% of errors over 3px, around 10mm.

The magnitude of these errors is thought to be increased by limiting factors of the camera used. The images were slightly out of focus, which proved very detrimental to edge detection. Additionally, if an infrared filter were used, edge clarification is likely by reducing blooming and pixel bleeding in the camera. It is anticipated that using a higher quality camera that is in focus and equipped with an IR filter, the error distribution could be shifted towards smaller errors. In addition to this, because the worst errors occur very infrequently, application of simple data filtering would aid in reducing the magnitude of these errors. It is predicted that for an industrial camera system as described in section 2.2, measurement accuracy could be within 5mm with 90% confidence.

### 3 Conclusions

This paper describes of a system designed to measure the off-centre position of a steel strip during rolling in the hot strip mill. Two main aspects of the system were presented, the hardware and the software. The design of the system was challenged by the harsh environment of the mill, with temperature, water, steam and dirt being the main obstacles.

The main challenge of the hardware design and choice was robustness and reliability. The components were all chosen for their effectiveness in harsh environments. The task was achieved by utilising water cooling and air barriers for cameras, and the Gigabit Ethernet protocol for data transmission, combined with a dedicated real-time computer. The physical aspects to the system design could therefore cope with the aggressive conditions.

The image analysis software had the task of seeing the edge of the strip though a considerable amount of steam and spray obscuring the view. Techniques were developed based around fitting a cubic Bezier curve to the strip edge and using predictive methods to filter noise from the images for enhancing measurement ability. Variable limitations on the position and shape of the curve and

tolerance of the prediction limits allow fine-tuning of the method for the application. By applying these techniques to the image analysis process, position measurement errors have been estimated to be less than 5mm.

Overall, the described system combines sturdy equipment, designed for the aggressive environment in a steelworks with a robust image analysis program to cope with noisy images and a less than ideal measurement target.

## 4 References

- [1] T. Kiyota, H. Matsumoto, Y. Adachi, E. Konda, Y. Tsuji and S. Aso, “*Tail crash control in hot strip mill by LQR*”, Proc. Amer. Control Conf., Denver, June 2003.
- [2] Y. Okamura and I Hoshino, “*State feedback control of the strip steering for aluminium hot rolling mills*”, Control Eng. Practice, vol. 5, 1997.
- [3] I. Mallocci, J. Daafouz, C. Iung, R. Bonidal and P. Szczepanski, “*Switched system modelling and robust steering control of the tail end phase in a hot strip mill*”, Nonlinear Analysis: Hybrid Systems, vol. 3, 2009.
- [4] J. de Roo, “*Theoretical background of strip-tracking and simulations with a strip-tracking model*”, unpublished, Corus, 2008
- [5] P. O’Leary, “*Machine vision for feedback control in a steel rolling mill*”, Computers in Industry, vol. 56, 2005
- [6] R. J. Montague, J. Watton, K. J. Brown, “*A machine vision measurement of slab camber in hot strip rolling*”, J. Materials Processing Technology, vol. 168, 2005.
- [7] Basler Vision Technologies, “*The Elements of GigE Vision*”, White Paper, accessed 10/07/2009
- [8] National Instruments “*PXI – National Instruments*” ([www.ni.com/PXI](http://www.ni.com/PXI)), accessed 30/07/2009
- [9] VideoTec “*NXW*” ([http://www.videotec.com/en/page\\_208.html](http://www.videotec.com/en/page_208.html)), accessed 30/07/2009
- [10] Carruthers-Watt, B., “*Application of Cameras to Measure Strip Tracking Position*”, unpublished, Corus, 2008
- [11] de Roo, J., “*Simulation of automatic tilt control in a 7 stand finish mill: Control by using a limited amount of CCD cameras*”, unpublished, Corus 2009
- [12] Cohen, E. et al., “*Geometric Modelling with Splines*”, Natick, A.K. Peters 2001
- [13] Kreyszig, E. “*Advanced Engineering Mathematics*”, New York, Wiley 1999